Final Report

Investigating the Underlying Mechanisms and Predictability of the MJO - NAM Linkage in the NMME Phase-2 Models

1. General Information

Project Title

Investigating the Underlying Mechanisms and Predictability of the MJO - NAM Linkage in the NMME Phase-2 Models

PI/co-PI Names and Institutions

- **Lead PI:** Jason C. Furtado, School of Meteorology, University of Oklahoma
- **Co-PI:** Elizabeth A. Barnes, Department of Atmospheric Sciences, Colorado State University
- **Co-PI:** Michelle L'Heureux, NOAA Climate Prediction Center
- **Co-PI:** Adam Allgood, NOAA Climate Prediction Center

Other Personnel

- Matthew Green, M.S. Student, School of Meteorology, University of Oklahoma
- Kirstin Harnos, Innovim LLC, Contractor, NOAA Climate Prediction Center.
- Laura Ciasto, Innovim LLC, Contractor, NOAA Climate Prediction Center.
- Imme Ebert-Uphoff, Research Professor, Department of Electrical and Computer Engineering, Colorado State University
- Savini Samarasinghe, Ph.D. Student, Department of Electrical and Computer Engineering, Colorado State University

Grant #: NA16OAR4310090

2. Main Goals of the Project, as Outlined in the Funded Proposal

- Enhance our knowledge about the dynamical links between the Madden Julian Oscillation (MJO) and the Northern Annular Mode (NAM) by considering the modulating influence of the extratropical stratosphere / stratospheric polar vortex (SPV).
- Evaluate these mechanisms of MJO-Northern Hemisphere (NH) extratropical atmospheric teleconnections in the North American Multi-Model Ensemble Phase-2 (NMME-2) system.
- Connect and apply our findings and evaluations to predictions of atmospheric blocking and extreme weather events.

3. Results and Accomplishments

INTRODUCTION

This project explored the joint influence that two major modes of subseasonal winter weather variability for the Northern Hemisphere (NH) – the Madden Julian Oscillation (MJO) and the Northern Annular Mode (NAM) – had on winter weather regimes across primarily North America and Europe. In particular, we were interested in understanding the interplay between MJO and variability in the stratospheric polar vortex (SPV), which also has a significant downward influence on the extratropical polar jet stream (i.e., storm tracks). This approach is ***new and novel***, as subseasonal forecasters traditionally consider each mode and its effect on the extratropical atmosphere *separately*. The guiding hypothesis for our project – ***the MJO-stratosphere***

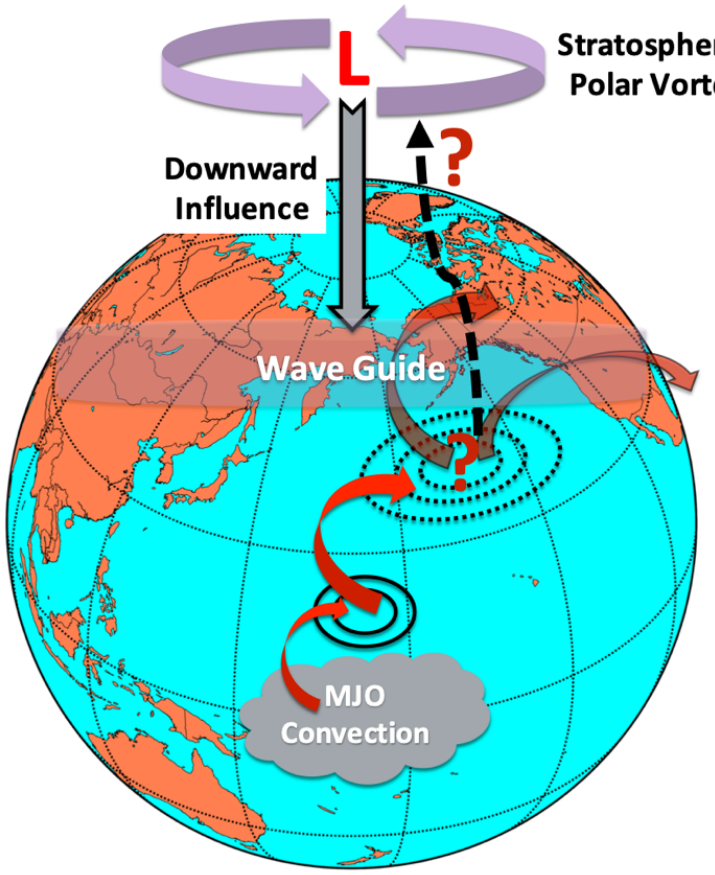

FIG. 1. Schematic of the guiding hypothesis for the project. Red arrows denote horizontal propagation of Rossby wavetrains initiated by MJO convection, while black arrows denote their vertical propagation. Red question marks denote uncertain effects on the wave propagation and magnitude.

modulation effect - is summarized in **Figure 1.** In brief, because the MJO's influence on the NH extratropics is through excitation of Rossby wavetrains, and the tropospheric waveguide is at least partially influenced by the state of the SPV vortex, it follows logically that the pre-existing state of the SPV can affect the MJO-induced teleconnections. The overall result from this modulation effect is a different downstream response in the expected interaction of the MJO with the NAM or its Atlantic representation the North Atlantic Oscillation (NAO), resulting in different weather regimes for North America and Eurasia than when considering *only* the MJO or *only* the SPV. Hence, the dynamic modulation of the MJO teleconnection by the state of the SPV represents a new predictor for subseasonal forecasting.

The results presented below are a summary of our work for this project, which mainly consisted of evaluating our hypothesis in reanalysis products (**Task #1)** and assessed important links in subseasonal-to-seasonal (S2S) model hindcasts in the S2S database [**Task #2;** *Vitart et al.*, 2017]. Unfortunately, we were unable to complete **Task #3** of the proposed work (i.e., evaluate the skill of the S2S models to replicate and capture observed MJO/SPV interaction events). Nevertheless, our findings were published in two (2) journal articles and presented at several conferences. In addition, the team also contributed their findings to the NOAA S2S Task Force Summary Document.

TASK #1: JOINT INFLUENCE OF THE MJO AND SPV ON WINTER WEATHER REGIMES (LEAD: FURTADO)

Lead PI Furtado and his graduate student **M. Green** used reanalysis data to investigate how different weather variables (e.g., 500 hPa geopotential heights (GPH), surface air temperature (SAT), and zonal winds) change depending on events when there was an active MJO and strong/weak SPV versus when only considering each mode separately. Thus far, most of the climate and S2S forecasting literature focused on examining the influence of the SPV and MJO on the extratropical flow pattern separately. However, in reality, these two modes (and others) work jointly to shape the NH wintertime tropospheric circulation. The findings of our work, published in *Green and Furtado* [2019], can now be used operationally to improve predictability of wintertime temperature and precipitation regimes across the Northern Hemisphere. This element of our work focused on answering two key research questions:

1. How do mean NH extratropical weather patterns differ when considering *only* the MJO, *only* the SPV, and *both*?
2. Do the MJO and the SPV work independently of one another to influence weather patterns, or are they acting on one another first?

Data and Methods

For this section of work, we use reanalysis data from ERA-Interim [*Dee et al.*, 2011] from 1979 to 2017. The main atmospheric fields are on a 1.5° by 1.5° horizontal grid and on 23 vertical pressure levels. Analyses are restricted to the extended boreal cold season (October – March), as these are the months when the MJO actively interacts with the NH extratropical circulation *and* also the active season for NH stratosphere-troposphere dynamical coupling. For the MJO, we use the Outgoing Longwave Radiation MJO index [OMI; *Kiladis et al.*, 2014]. The phase and amplitude are derived from the OMI in a similar manner set forth by *Wheeler and Hendon* [2004]. We group results into MJO Phases 2 and 3 (i.e., active convection in the Indian Ocean / suppressed convection in the western / central tropical Pacific) and Phases 7 and 8 (active convection in the central tropical Pacific / suppressed convection in the Indian Ocean). This grouping is also done to increase sample sizes for our composite analyses. To characterize the state of the SPV, we use the phase and magnitude of the NAM index at 100 hPa (NAM_{100}). This pressure level captures SPV events that are most likely to propagate down into and affect the troposphere. Conclusions of the study are robust (albeit with some different events) when using NAM_{50} to define events.

For our composites, we use the following definitions. The start date for an *MJO event* in when the MJO is in a particular phase, $|OMI| \geq 1\sigma$, and remains above this threshold for three (3) consecutive days. The start date for a *strong (weak) SPV event* is when $NAM_{100} \geq 1\sigma$ ($NAM_{100} \leq -1\sigma$) *and* the same sign for five (5) consecutive days. Neutral cases for the MJO and SPV are categorized when the magnitude of the corresponding index is less than 1σ. Joint composite cases are categorized as: (a) MJO Phases 2 and 3 + weak SPV; (b) MJO Phases 2 and 3 + strong SPV; (c) MJO Phases 7 and 8 + weak SPV; and (d) MJO Phase 7 and 8 + strong SPV. In addition to joint events, we also consider times when each event happens independently while the other mode is neutral; i.e.,

- An *MJO X + Neutral SPV event* occurs when $|OMI| \geq 1\sigma$ in phase X, but $|NAM_{100}| < 1\sigma$.
- A *Strong SPV + Neutral MJO event* occurs when $NAM_{100} \geq 1\sigma$ but the MJO is neutral.
- A *Weak SPV + Neutral MJO event* occurs when $NAM_{100} \leq -1\sigma$ but the MJO is neutral.

Table 1 shows the number of events for each composite category.

TABLE 1. Number of events for each of the individual and joint composite cases.

	Neutral SPV	**Weak SPV**	**Strong SPV**
Neutral MJO		37	43
MJO Phase 2 and 3	68	23	21
MJO Phase 7 and 8	69	18	18

For this study, we examine GPH and SAT primarily with lags +10 to +14 days after the start date of the event. This 5-day average represents the time just into the subseasonal range. Despite the propagation nature of the MJO, we consider the phase of the MJO on Day 0 only for categorizing the single and joint composites presented. Statistical significance ($p < 0.05$) for our statistical analyses is assessed using a two-tailed bootstrapping of $N = 5{,}000$ samples with replacement.

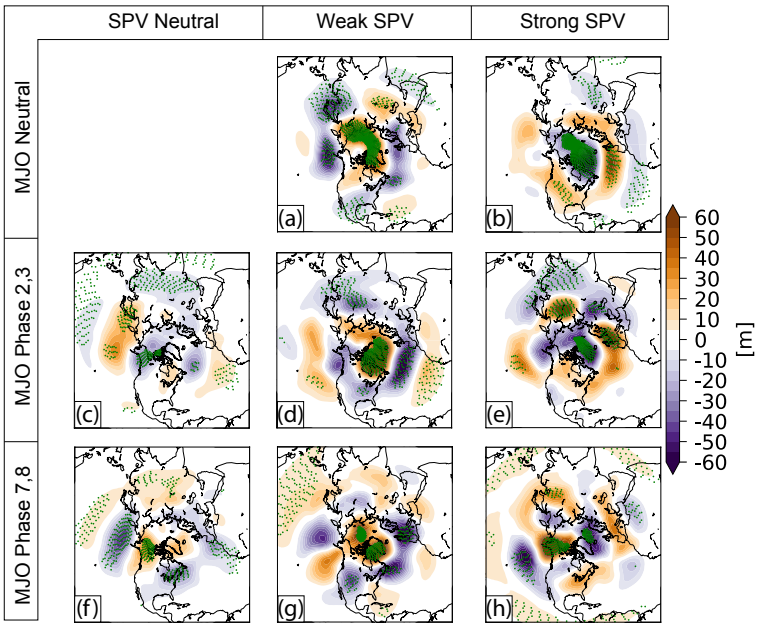

FIG. 2. Lag composite (+10 to +14 days) of 500 hPa GPH anomalies (m) for the various MJO + SPV cases. Green stippling indicates anomalies which are significant ($p < 0.05$) using a two-tailed bootstrapping test of $N = 5000$ samples with replacement.

Results: GPH and SAT Composites

We start with examining the mid-tropospheric circulation field with composites of 500 hPa GPH anomalies for the various composite cases (**Figure 2**). The neutral case composites reproduce familiar patterns seen in previous studies for the single indices. Specifically, weak SPV + neutral MJO (**Fig. 2a**) and strong SPV + neutral MJO composite (**Fig. 2b**) means capture the characteristic negative and positive NAM tropospheric circulation patterns, respectively. The MJO Phase 2,3 + neutral SPV **(Fig. 2c**) and MJO Phase 7,8 + neutral SPV (**Fig. 2f**) display the canonical Rossby wavetrain emanating from the tropics across North America and into the North Atlantic. Turning to the conditional composites, in the MJO Phase 2,3 + weak SPV case (**Fig. 1d**), ridging typically over the northwest Pacific during MJO Phase 2,3 conditions (**Fig. 1c**) shifts eastward with significant troughing seen across Alaska, while conditions resemble negative NAO conditions in the Atlantic. A similar story emerges for the MJO Phase 2,3 + strong SPV composite (**Fig. 2e**) – i.e., the Pacific sector resembles more of the MJO Phase 2,3 signature while the Atlantic sector captures the downward influence of the strong SPV via a positive NAO signature. For the MJO Phase 7,8 + weak SPV cases (**Fig. 2g**), constructive interference between the two modes occurs over the NH except in North America, where ridging in the southeastern US replaces the characteristic trough over eastern North America seen during weak SPV episodes (**Fig. 2a**) northwestward. Importantly, over the North Atlantic, a negative NAM/NAO signature again emerges. This constitutes the first major finding of our study: ***the state of the SPV and its influence on the tropospheric NAM better represents circulation patterns across most of Eurasia versus the MJO or the MJO + SPV conditional composites.*** By contrast, the MJO Phase 7,8 + strong SPV cases (**Fig. 1h**) show large-scale *destructive interference* between the two modes across the hemisphere.

The idea of constructive versus destructive interference between these modes is best captured by examining spatial correlations between the different composite maps for the entire NH and four specific sectors: the North Pacific (20°-60°N, 150°E – 140°W), North America (20°-60°N, 60°-120°W), the North Atlantic (20°-75°N, 60°W - 20°E), and Eurasia (20°-75°N, 30°-130°E). **Figure 3** presents these spatial correlations for the different joint cases and regions. The MJO Phase 7,8 + weak SPV composite-mean 500 hPa GPH field exhibits statistically significant ($p <$

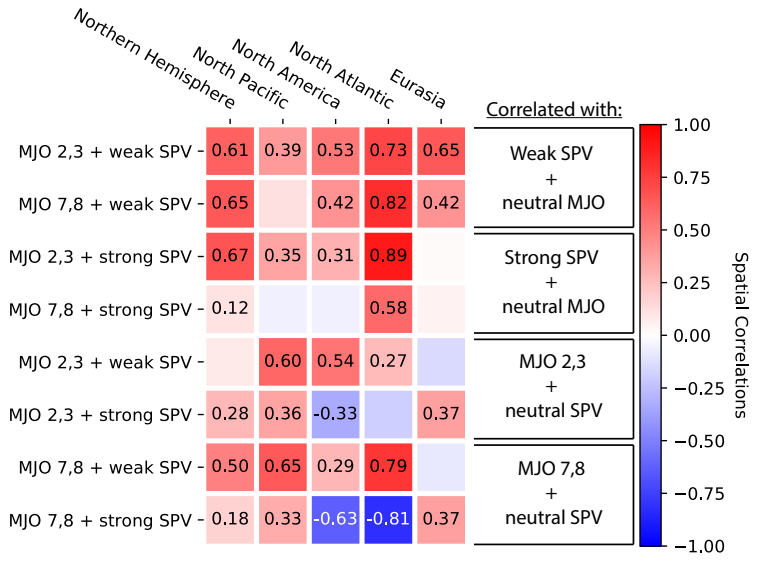

FIG. 3. Spatial correlation coefficients of MJO + SPV neutral composites against various conditional MJO + SPV cases. Correlations done for five specific regions. Significant correlation coefficients ($p < 0.05$) explicitly shown in the heat map.

0.05) positive correlations with the weak SPV + neutral MJO composite-mean pattern over all areas except the North Pacific. By contrast, when comparing the MJO Phase 7,8 + strong SPV to the MJO Phase 7,8 + neutral composite-means, the pattern correlations are significantly *negative*, showing strong destructive interference. Constructive interference also occurs for MJO Phase 2,3 + strong SPV and strong SPV + neutral MJO composites (**Fig. 3**), as described above.

Turning to sensible weather, **Figure 4** shows composites for SAT anomalies for the various cases. In all conditional composite cases, SAT anomalies across Europe and most of Asia resemble the SAT anomalies expected when considering only the state of the SPV (e.g., compare **Figs. 4d and 4g** with **Fig. 4a** and **Figs. 4e and 4h** with **Fig. 4b**). However, a different story emerges for North America. Here, we see considerable variance between the conditional composites when compared to either of the single-index composites. For example, both the Weak SPV + neutral MJO (**Fig. 4a**) and the MJO Phase 7,8 + neutral SPV (**Fig. 4f**) composites show the propensity for cold SAT anomalies across much of the eastern half of North America. However, for the MJO Phase 7,8 + weak SPV cases (**Fig. 4g**), significant cold anomalies only appear across far northeastern North America, with *warm* anomalies across the Southeast and Mid-Atlantic US. ***Therefore, from a forecasting perspective, considering both the state of the SPV and the phase of the MJO could change forecast rationale for wintertime temperature predictions across North America.***

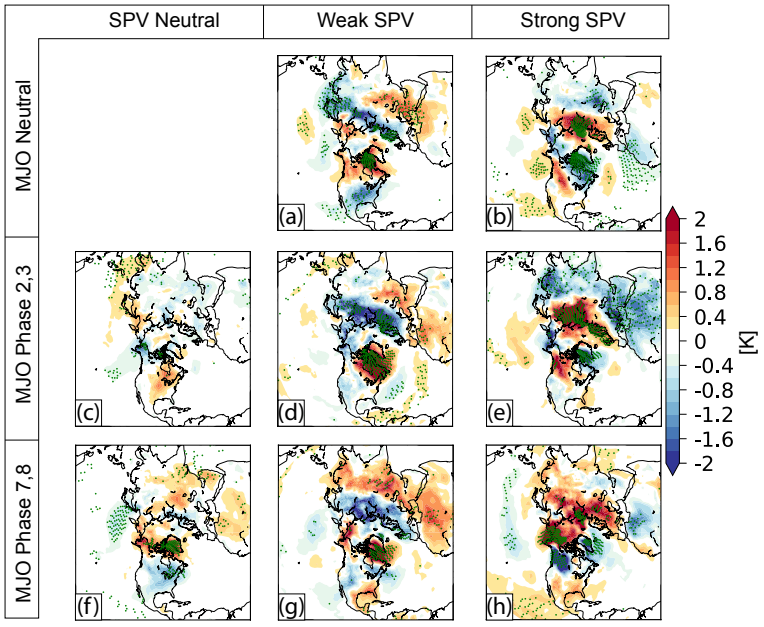

FIG. 4. As in **FIG. 2** but for SAT anomalies (K).

Results: Stratosphere-Troposphere Coupling Metrics

The composite analyses presented in the past section of show significantly different patterns across the NH for different MJO/SPV cases, supporting our initial hypothesis of including both modes for subseasonal boreal winter forecasting applications. Next, we examine whether vertically propagating Rossby waves exhibit different characteristics depending

on the various composite cases. **Figure 5** presents the Day +10 to +14-averaged Eliassen-Palm (EP) fluxes and flux divergence for our various cases. The two SPV + neutral MJO cases agree with the results by *Thompson et al.* [2006], which show how a weak (strong) SPV can reorganize tropospheric eddies to shift the polar jet stream equatorward (poleward) by pumping westerly momentum equatorward (poleward) (**Figs. 5a and 5b**). By contrast, there are no substantial EP-flux anomalies in the stratosphere during MJO Phase 2,3 + neutral SPV cases (**Fig. 5c**). This result suggests that the MJO Phase 2,3 influences the tropospheric NAM primarily via ***a tropospheric pathway.***

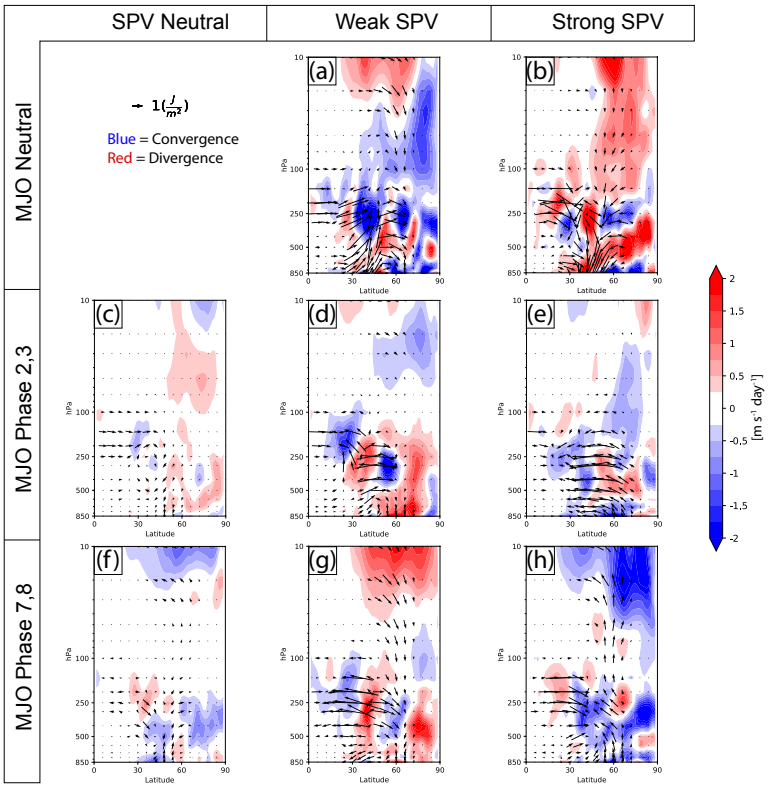

FIG. 5. Lag composite (+10 to +14 days) of Eliassen Palm (EP) fluxes (vectors; J m^{-2}) and flux convergence (shading; m/s/day) anomalies for the various MJO + SPV conditional composites. Shaded contour interval 0.25 m/s/day; zero contour omitted. Vectors scaled as in *Edmon et al.*, [1980].

Conclusions change for events involving MJO Phase 7,8. In the MJO Phase 7,8 + weak SPV events (**Fig. 5g**), similar patterns to that of the weak SPV + neutral MJO are visible – i.e., anomalous downward wave propagation in the stratosphere and troposphere from about 60°N poleward. This anomalous wave propagation leads to strong flux divergence in the mid-lower stratosphere, indicating a strengthening SPV. The patterns of the MJO Phase 7,8 + strong SPV events (**Fig. 5h**) are essentially opposite to those of the strong SPV + neutral MJO case (**Fig. 5b**), with anomalous *convergence* in the polar stratosphere leading to a breakdown or weakening of the SPV. Hence, both of these composites suggest that the MJO Phase 7,8 relationship with the tropospheric NAM acts ***both with a tropospheric and a stratospheric pathway.***

Finally, we invesigate whether the MJO and the SPV can work independently from one another to influence NH winter weather patterns or if the MJO acts to influence the SPV first. To do so, we analyze how pressure-lag composites of the NAM index change for MJO + neutral SPV events (**Figures 6** and **7**). For the MJO Phase 2,3 + neutral SPV composite (**Fig. 6a**), negative NAM conditions exist in the troposphere *before* Day 0 and are significant around Days -12 to -8. Then, a significant *positive* tropospheric NAM signature emerges, extending up into the stratosphere and yielding anomalously strong zonal winds (**Fig. 6b**). For the MJO Phase 7,8 + neutral SPV composite cases (**Fig. 7a**), the trend after Day 0 is toward negative NAM in the troposphere (significant for Days +8 to +16), with the stratospheric NAM turning more negative after the tropospheric NAM has reached its peak negative value (see green box in **Fig. 7a**). This evolution makes sense from the anomalous wave propagation depicted in **Fig. 5f**, where the MJO

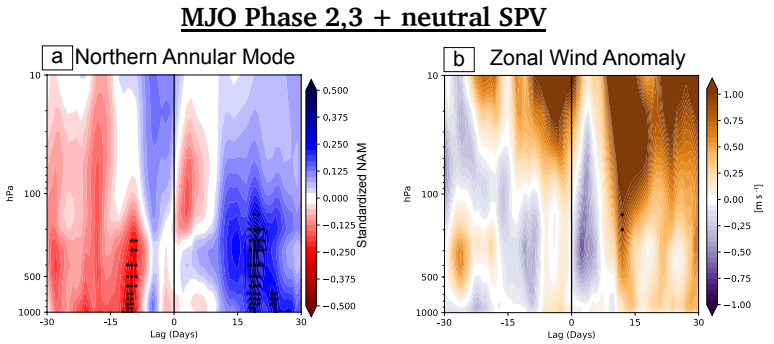

FIG. 6. Pressure-time lag composites of (a) standardized NAM index and (b) area-averaged (60°-80°N) zonal-mean zonal wind anomalies (m/s) for MJO Phase 2,3 + neutral SPV events. Day 0 represents the start date of the MJO event (black vertical line in both plots). Negative (positive) lags indicate the variable leads (lags) the start of the MJO event. Black stippling indicates composite values significant at the $p < 0.05$ level using a two-tailed bootstrapping test of $N = 5000$ samples with replacement.

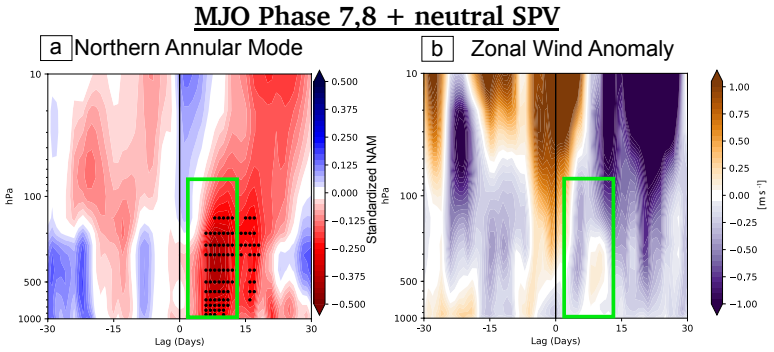

FIG. 7. As in **FIG. 6** but for MJO Phase 7,8 + neutral SPV.

Phases 7,8 events change the tropospheric Rossby wave sources, which then propagate vertically and converge in the stratosphere, weakening the vortex (see also **Fig. 7b**).

Conclusions

The three main conclusions of this part of the project are:

1. The MJO strongly influences patterns across the North Pacific and western North America, while SPV variability dominates tropospheric weather patterns over the North Atlantic and Europe. North America winter weather patterns depend on knowing the phase and amplitude of both modes.

2. MJO influences on the extratropical stratospheric circulation may be contingent on the state of the SPV, especially for MJO Phases 7,8.

3. MJO Phase 2,3 + neutral SPV events are associated with a strengthening SPV, while MJO Phase 7,8 + neutral SPV events are associated with a weakening of the SPV. The impacts of the MJO on the tropospheric circulation can be via a tropospheric or tropospheric *and* stratospheric pathway.

Repeating our analyses using multi-linear regression for the MJO and SPV do *not* yield the same patterns and differences. Hence, the joint influences of the MJO and SPV are *not simply linear*. Overall, the results of our composite analyses increase the range of possibilities for long-range forecasts and highlight which areas of the hemisphere are more related to the MJO or the SPV to enhance forecast skill.

CAUSAL DISCOVERY AND MJO-NAM/NAO RELATIONSHIPS (TASK #1) (LEAD: BARNES)

Co-PI Barnes, investigators **I. Ebert-Uphoff** and **S. Samarasinghe**, and **PI Furtado** performed novel research examining the causal links between the MJO, SPV, and the NAM / NAO. As already discussed in the last section, variability in the tropospheric NAM arises several sources, including the MJO and the SPV. However, the exact interactions between these multiple pieces are complex and difficult to disentangle at times. This result is especially complicated because of the tropospheric and stratospheric pathways through which the MJO can impact the tropospheric NAM/NAO. Therefore, traditional climate dynamics statistical techniques like lagged regressions and composites cannot adequately disentangle the interplay between these modes. Hence, the team decided to use ***causal discovery theory*** to find the different pathways at work and also

calculate the time lags associated with the interactions of these three modes. The results of the work are published in *Barnes et al.* [2019] and are summarized below.

Data and Methods

The three main indices used in this part of the work are: (1) ***The MJO Index***, based on the Real-time Multivariate Index (RMM) from *Wheeler and Hendon* [2004]; (2) ***The SPV (or VORTEX) Index***, based on daily 100 hPa GPH (area-averaged poleward of 60°N) from ERA-Interim; and (3) ***The NAO Index,*** which are daily-mean values downloaded from the NOAA Climate Prediction Center. Additional testing was done for a VORTEX index at 50 hPa, and the conclusions of this study were similar (not shown). While the MJO index is treated as a binary index (1 for an event, 0 for no event), the NAO and VORTEX indices have three possible values: -1 (i.e., a negative NAO/weak SPV), 0 (neutral NAO/SPV) and +1 (positive NAO / strong SPV). Indices are considered during the extended cold season (October – April) over the period 1979 – 2016. A 5-day running-mean is applied to the VORTEX and NAO indices to smooth out synoptic noise.

Causal discovery theory is the main technique used in this work, which relies on graphical theory [e.g., *Chu et al.*, 2005; *Ebert-Uphoff & Deng*, 2012; *Runge et al.*, 2015]. This method identifies only *direct* causal relationships, and the determination between these direct links and indirect links are a key feature of causal discovery theory. Moreover, this theory identifies *potential* causal relationships from which we can generate hypotheses for further testing. It does not prove such relationships. For our purposes, we consider three variables: the MJO, VORTEX, and NAO. Moreover, because of the multiple phases of the MJO, the study considered four distinct causal discovery graphs for the following groupings: MJO Phase 2/3, 4/5, 6/7, and 8/1.

Results: "Traditional" Lagged Composites

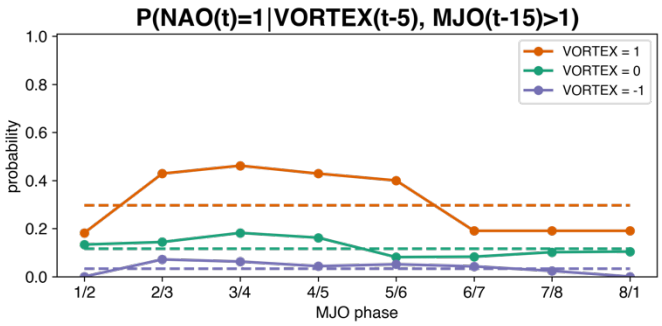

FIG. 8. (solid lines) Probability (i.e., fraction of days) that the NAO = 1, 15 days following different MJO phases and various VORTEX conditions: VORTEX = 1 (orange), VORTEX = 0 (green), and VORTEX = -1 (blue). (dashed lines) Probability that NAO = 1 for non-active MJO periods for the same colored VORTEX cases.

Before presenting the results from the causal discovery graphs, we present initial findings using conditional probabilities. **Figure 8** shows the probability that the NAO index will be positive (i.e., greater than 1) as a function of MJO phase 15 days ahead of time and for a given different state of the SPV 5 days ahead of time. Regardless of the phase of the MJO, the NAO has a higher probability of being positive when the SPV is strong 5 days before (**Fig. 8**, dashed orange line) compared to when the SPV is neutral or weak (**Fig. 8**, dashed purple and green lines). Moreover, when partitioning these base probabilities by MJO phase, the NAO is more likely to be positive 15 days following MJO Phases 2/3, 3/4, and 5/6. Hence, conditioning the state of the SPV on the phase of the MJO ***increases our forecast confidence of a positive NAO regime***. This finding supports the findings from *Green and Furtado* [2019]. Indeed, the important part of **Fig. 8** is the difference between the solid and the dashed lines, as that difference represents the ***additional information we are gaining by considering the MJO phase along with the state of the SPV.***

To further highlight the conditional probabilities for different phases of the MJO and VORTEX states, **Figure 9** presents tables of the average value of the NAO as a function of lead time and phase of the MJO. The probabilities are further partitioned by the state of the SPV. Considering

the case when the SPV is strong (i.e., VORTEX = 1; **Fig. 9a**), the entire probability table is red, indicating a positive NAO. Hence, no matter the lead or phase of the MJO, the NAO is overall positive when the SPV is strong. Note that this is even true when the MJO is inactive (**Fig. 9a**, leftmost column). Looking closely, we see a less positive stripe of NAO values for Phases 6/7 – 8/1 for leads of 20+ days, indicating a slight lagged influence that could result in less positive or even at times negative NAO conditions in some cases. Likewise, when the SPV is weak, the NAO is mostly in a negative state (**Fig. 9c**), though there is some variety. In particular, there is a stripe of positive NAO values for Lags 15-20 for MJO Phases 2/3 and even 3/4. These results make sense from previous literature [e.g., *L'Heureux and Higgins*, 2008]. When the SPV is in a neutral state (**Fig. 9b**), the average values of the NAO are still overwhelming positive in most cases. However, the values are much smaller and even close to 0 in some cases, suggesting lots of variability for the NAO under neutral SPV conditions. Additionally, weakly *negative* NAO values appear in a diagonal stripe from MJO Phase 5/6 and Lag +20 days down to MJO Phase 8/1 at Lag +5, agreeing again with *L'Heureux and Higgins* [2008] and *Cassou* [2008].

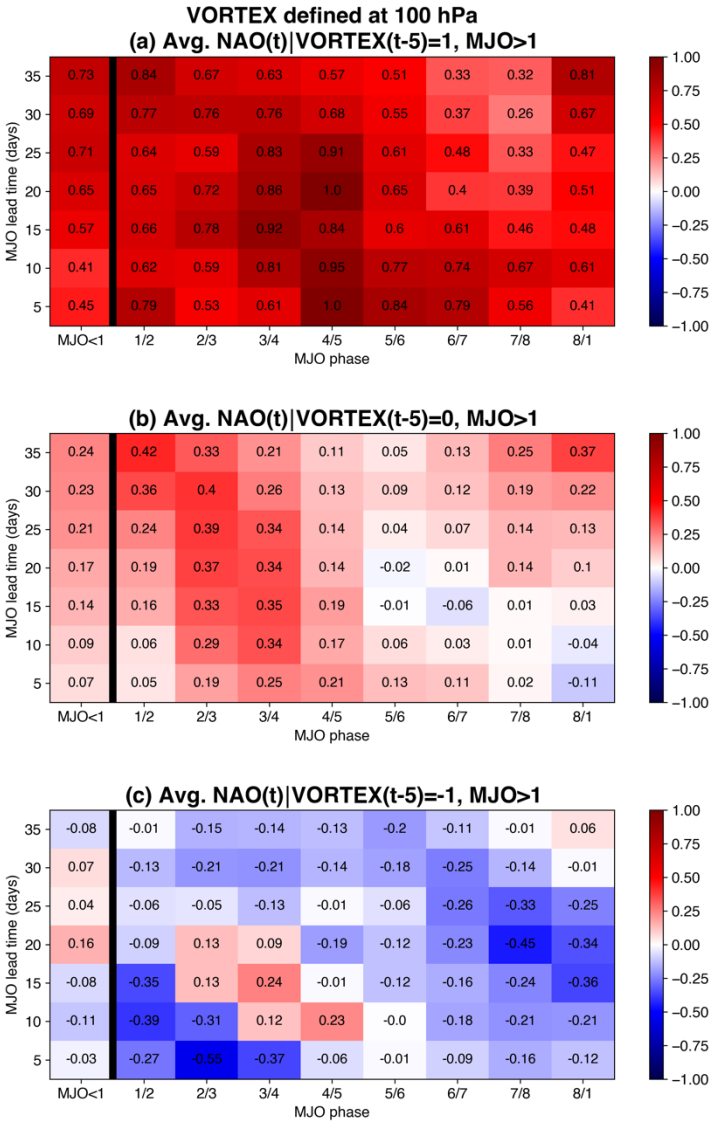

FIG. 9. The average NAO index (shading and numerical values) for various lead times and various phases of the MJO. Probabilities further conditioned by the state of the SPV 5 days earlier: (a) VORTEX = 1, (b) VORTEX = 0, and (c) VORTEX = -1. Leftmost column denotes probabilities when the MJO is inactive.

Results: Causal Discovery Theory

Although **Figs. 8** and **9** present compelling evidence supporting the central hypothesis of our work, they rely on "traditional" statistical methods. The novel aspect of this particular work is using causal discovery theory. **Figure 10** highlights the significant findings of the work via causal summary graphs. In these graphs, the arrows denote the direction of potential cause-effect relationships, looped arrows denote autocorrelations, and the bolded numbers indicate the significant lags at which these relationships exist. The three major results from these graphs are:

1. There are two clear causal pathways from the MJO to the NAO: (a) A direct one, and (b) an indirect one: the MJO to the SPV and then downward to the NAO.

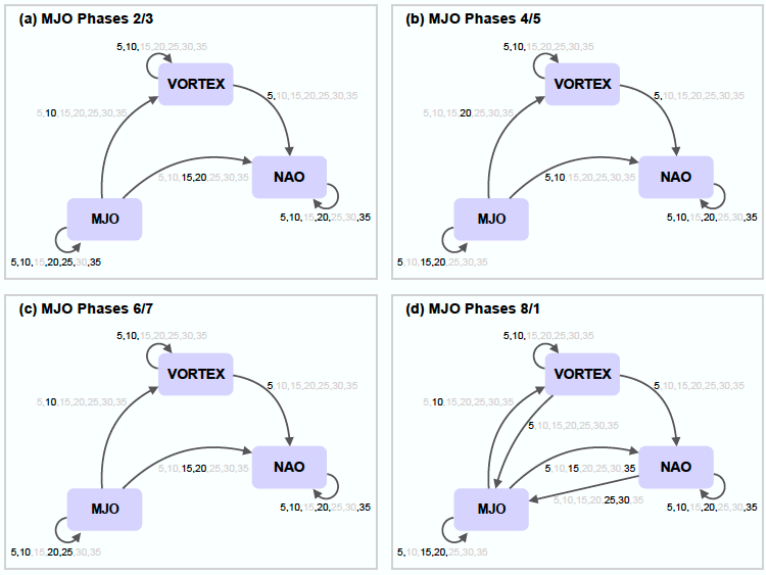

FIG. 10. Summary graphs of the causal links segmented by MJO phases: (a) Phases 2/3; (b) Phases 4/5; (c) Phases 6/7; and (d) Phases 8/1. Bolded numbers indicate significant lags for the causal relationship; gray numbers indicate lags with insignificant causal relationships.

2. A change of the state of the SPV may cause a change of the NAO 5 days later. Likewise, MJO Phases 2/3 (**Fig. 10a**) may causally affect the NAO at a delay of 15-20 days, with no significant connections at any of the other lead times.

3. The MJO phases 8/1 graph (**Fig. 10d**) includes feedback loops from NAO to MJO and from VORTEX to MJO that are not identified for any of the other phases. The direct causal influence of the NAO is on MJO phases 8/1 at a lead of 25-30 days, although further analysis indicates that this direct connection is only strong for Phase 8 (not shown).

The graphs in **Figure 10** only include arrows for direct connections, but we can infer indirect connections. For example, although the MJO might affect the NAO 15–20 days later, there may be indirect effects that last much longer due to autocorrelation (**Fig. 10**, looped arrows). Indeed, **Fig. 10a** indicates that the MJO may be highly predictive of the NAO state 5, 10, 20, and 35 days ***after*** those initial 15–20 days. Hence, these graphs highlight the true causal pathways that are responsible for the combined effects, but are not necessarily good to use for predictive models. To do that, we would need to untangle the direct and indirect pathways presented in these diagrams. Results from **Figs. 8** and **9** would be more appropriate for use in prediction models.

Conclusions

Taken together, the results of the section of our project present an important step forward in understanding MJO/NAO interactions and how the SPV can modulate this effect. Both methods show that the MJO impacts the NAO via a tropospheric pathway *and* a stratospheric pathway, as illustrated before. Indeed, the MJO influences the strength of the stratospheric polar vortex on a timescale of~10 days, and then 5 days later the vortex drives changes in the NAO. Additionally, the SPV conditions the tropospheric circulation to be conducive (or not) to the influence of the MJO. For example, the NAO responds to the MJO when the SPV is the same sign as the NAO response (i.e., NAO positive for a strong SPV / NAO negative for a negative SPV). This knowledge could be useful in S2S forecasting applications for the NAM/NAO and thus improve our skill when predicting winter weather regimes across Europe especially and even parts of North America.

MJO-NAM Relationships in S2S Models (Task #2) (Lead: L'Heureux and Ciasto)

Co-PI L'Heureux and contractors **Ciasto** and **Harnos** examined and evaluated the MJO-SPV connections in hindcast simulations from the S2S model database [*Vitart et al.*, 2017]. A major benefit of this model database is that it includes models with a range of vertical levels and low-top as well as high-top models. This range of model configurations allows us to examine how vertical model resolution and model top influences the ability of the models to capture the stratospheric

role in MJO teleconnections to the extratropical NH. ***This characterization was a central tenet of the original NOAA MAPP.***

To that end, the analysis examines the following three questions:

1. Does the link between the MJO and the leading pattern of tropospheric variability (the Arctic Oscillation, AO, or tropospheric NAM) also exist with the leading pattern of SPV variability?
2. Does the state of the stratospheric circulation affect the tropospheric MJO-AO relationship?
3. How well are these relationships simulated in S2S prediction models?

Data and Methods

Verification of daily atmospheric fields originate from ERA-Interim over the period 1979-2016. Focus remains on the extended cold season (November-March; NDJFM). The three climate modes of interest – the AO/tropospheric NAM, the MJO, and the SPV – are defined as follows. Daily-mean values of the AO/NAM come directly from the NOAA CPC and are produced by projecting daily spatial maps of 1000 hPa geopotential height (GPH) anomalies onto the leading empirical orthogonal function (EOF) of NDJFM 1000 hPa GPH anomalies [i.e., the definition of the AO/tropospheric NAM; *Thompson and Wallace*, 2000]. Likewise, daily-mean values of the SPV index are created by projecting daily-mean anomalies of 50 hPa GPH onto the leading EOF of NDJFM 50 hPa GPH anomalies. The MJO index comes from the traditional RMM index [*Wheeler and Hendon*, 2004].

For the hindcasts, **Table 2** lists the models studied for this work. The simulated AO index is calculated for each S2S model by projecting the leading EOF of *observed* monthly 1000 hPa GPH anomalies onto the *simulated* daily 1000 hPa GPH anomalies at each forecast lead. Projecting the observed AO pattern onto the simulated anomalies ensures that all models describe the temporal evolution of the same spatial pattern. A similar method is used to calculate the simulated SPV index using 50 hPa GPH anomalies. The simulated RMM indices are obtained from the S2S website (https://s2sprediction.net).

TABLE 2. Description of S2S models used in the analysis. Note that a maximum of 4 ensemble members were used in the analysis. Values in parentheses correspond to the forecast sampling used for this analysis.

Model	Reforecast Period	Frequency	Ensemble Size	Vertical Levels	Model Top (hPa)
ECMWF	1996-2015	2/week (weekly)	11	91	0.01
CNRM	1993-2014	2/month	15	91	0.01
NCEP	1999-2010	Daily (6/month)	4	64	0.02
UKMO	1996-2009	4/month	3	85	85 km
JMA	1981-2010	3/month	5	60	0.1
ECCC	1995-2012	Weekly	4	40	2
HMCR	1985-2010	Weekly	10	28	5
BOM	1981-2013	6/month	33	17	10

Results: S2S Model Evaluation

We begin the evaluation of the S2S models and the MJO-AO relationship by assessing the anomaly correlations of the three indices during NDJFM within the S2S models, a measure of assessing the skill of the models at forecasting these indices. **Figure 11a** indicates that the models

the majority of the models are able to reproduce the daily AO index at short leads (less than 5 days). By day 10, the correlations of most models decreased to ~0.5-0.6, suggesting that the models are skillful at predicting the AO out to about a week at most (note that an anomaly correlation of 0.5-0.6 is usually taken as the "predictive skill" barrier). Relative to the AO, simulations of the SPV index exhibit greater anomaly correlations (**Fig. 11b**) with correlations greater than 0.9 out to at least 10 days, except in the JMA and BOM models. These results affirm the long persistence expected in stratospheric circulations. However, the models are much less skillful at predicting the magnitude of MJO events (**Fig. 11c**). *Vitart* [2017] illustrated that the S2S models are skillful at capturing the correct *phase* of the MJO – i.e., where the tropical convective dipole is located. This element is also confirmed in our work. Thus, the models are less capable of getting the actual magnitude of the event. ***This aspect is important, as the magnitude of the MJO event will affect the simulated relationship between the MJO and the NAM in the models.***

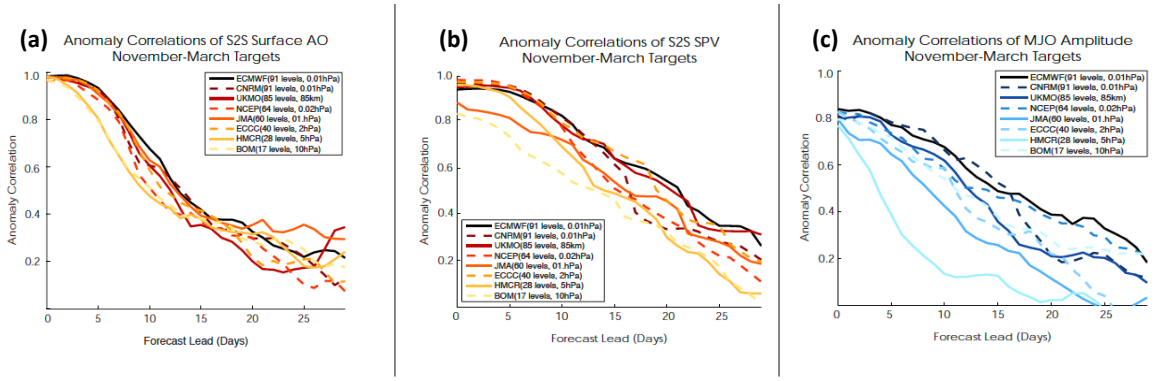

FIG. 11. Anomaly correlations between observed (i.e., from reanalysis) and simulated S2S indices for target days during NDJFM. Indices assessed are (a) AO/tropospheric NAM index, (b) SPV index, and (c) amplitude of the MJO (regardless of phase). Different lines denote results from each S2S model (see legend in each panel).

Figure 12 presents that the observed MJO-AO link (**Fig. 12a**), in which positive AO / tropospheric NAM days tend to dominate in MJO Phases 2-4 and negative AO days tend to dominate in MJO Phases 7-8, is well simulated the majority (6 to 7) of the 8 S2S models (**Fig. 12b**) and the subsampled observations (**Fig. 12b**, circles). These relationships are also evident at a forecast lead of 7 days but diminish significantly by 14 days. Taken together, the results indicate two key findings. First, the relationship between the sign of the AO and the phase of the MJO reflects a robust tropical-extratropical linkage that is evident in the full set of observations, subsampled observations and numerous prediction models. Second, these linkages are evident in the S2S models despite their poor skill at capturing the MJO amplitude (**Fig. 12c**). So, while the models might not capture the actual amplitude skillfully at long lead times, they ***might*** be able to still simulate MJO events exceeding an amplitude of 1.

Despite these findings, however, the overall relationships between the MJO and the SPV are harder to capture in the S2S models (**Figure 13**). The observations demonstrate that positive SPV days, like its tropospheric counterpart, tend to dominate during Phases 2-4 of the MJO (**Fig. 12a**). However, most models (or subsampled observations) fail to capture this relationship (**Fig. 12b**). This lack of a robust finding between the SPV and the MJO indicates that the S2S models may have some bias in the mean state of the NH extratropical stratospheric base state or stratosphere-troposphere dynamical coupling processes. The other possibility is that the limited sample size of the events considered could also skew the results

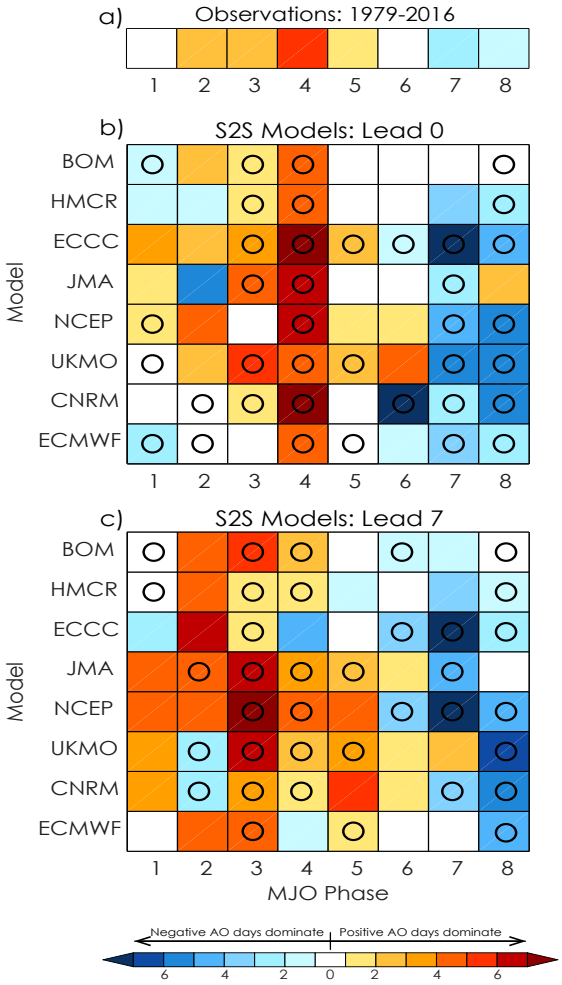

FIG. 12. Difference between the percentage of positive and negative AO days as function of MJO phase for (a) reanalysis, (b) S2S models at target lead 0 and (c) S2S models at target lead 7 days. Circles denote instances when the model and the subsampled observations (i.e., observations sampled to match the forecast starts of each model) agree on the sign of the AO dominance.

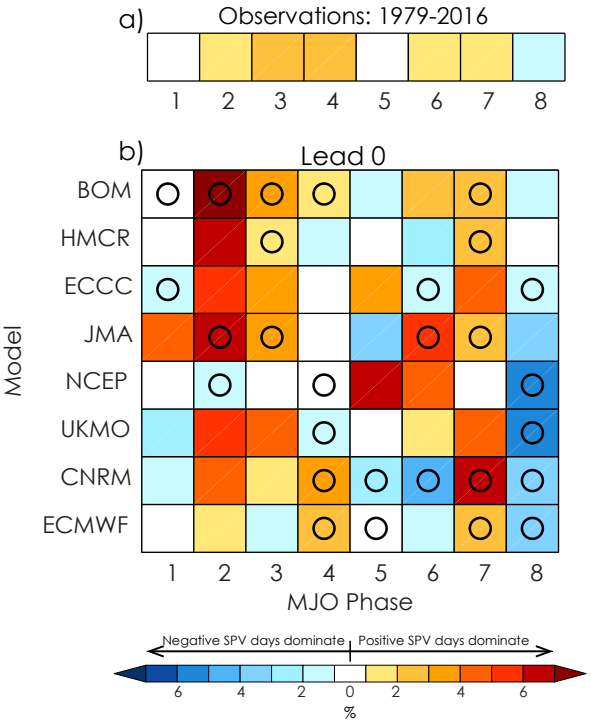

FIG. 13. As in (a) **FIG. 12a** and (b) **FIG. 12b** but for percentage of positive and negative SPV in each MJO phase.

Finally, we make direct comparisons between how the models recover observed surface temperature regimes associated with different MJO+SPV conditions via composite analyses similar to those in **Fig. 4** but using the S2S model hindcasts. **Figures 14** and **15** show the composite of SAT anomalies for leads 0-5 days following MJO Phases 2-4 (**Fig. 14**) and MJO Phases 7-8 (**Fig. 15**) for different SPV conditions. Results are shown for ERA-Interim (top row) and three select models (BOM, NCEP, and ECMWF). When the MJO is in phases 2-4 (**Fig. 14**), the models agree well with each other (bottom three rows) but less so with the re-analysis (top row), especially in the magnitude of the SAT anomalies. For example, during periods of anomalously strong SPV, the models, especially NCEP, suggest more widespread and stronger warming over the US. The models disagree most during weak SPV conditions, during which the NCEP composite presents more extensive cooling over the US and less warming over the Arctic. Joint composites for the MJO Phases 7-8 with the model simulations feature even less agreement with reanalysis (**Fig. 15**). Indeed, we find opposite signatures between the models and reanalysis, e.g., for NCEP during MJO

Phase 7,8 + neutral SPV events (**Fig. 15,** left column). For both MJO cases, the BOM recovers the observed relationships the best (**Figs. 14** and **15**, second row). Surprisingly, this model is also the one with the lowest model lid (10 hPa) and least number of vertical levels (17).

Conclusions

Our evaluation of the MJO-NAM connections and the MJO-stratosphere modulation hypothesis with the S2S models yielded mixed results. First, the tropospheric MJO-AO relationships – i.e., the relationship between MJO phases 2-4 (7-8) and the positive (negative) AO/tropospheric NAM – are robust features within the models. The links are best seen evidenced at short leads in almost all of the S2S models though fade at longer leads, in part because of the loss of forecast skill for the AO/tropospheric NAM. More analysis is needed with the models to more accurately capture the predictability scale of the near-surface NAM, especially when considering the stratosphere, a reservoir of low-frequency memory for the NH wintertime climate system. Secondly, the role of the stratospheric circulation in the MJO-AO links is harder to discern in the models. In most cases, the models could not fully capture the MJO relationship to the stratospheric circulation or the MJO-AO relationship under specific SPV conditions. In terms of predictability and the MJO-stratosphere modulation hypothesis, the results from the S2S models suggest that, even at target lead 0, the models have difficulty agreeing on the interactions between the SPV and the MJO phases and the associated SAT anomalies. However, the joint composites are more consistent between reanalysis and the models for MJO Phases 2-4, meaning that the models appear to simulate better teleconnections associated with anomalous convection over the Indian Ocean and the NH extratropical wintertime circulation. Reasons why the models perform less well

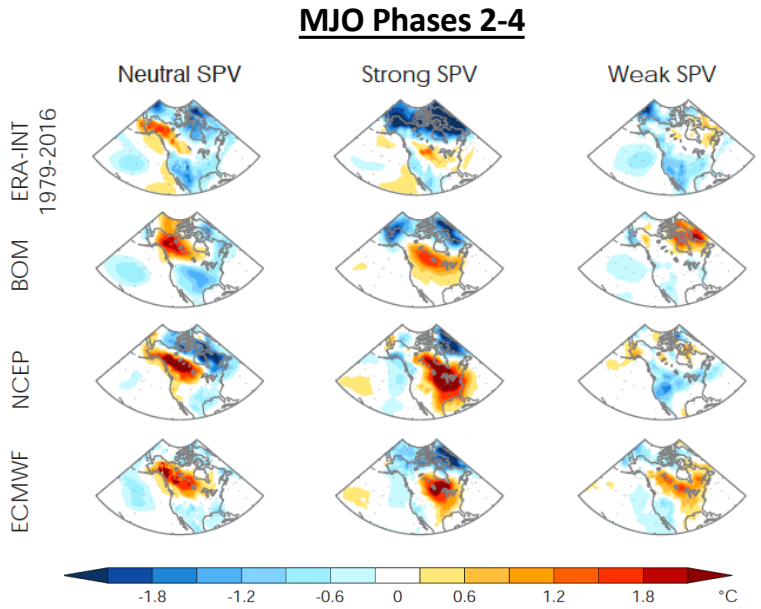

FIG. 14. Composite means of daily NDJFM SAT anomalies (°C) associated with times when the MJO in in phases 2-4 and the SPV index is (left) neutral, (middle) anomalously strong, and (right) anomalously weak. Results shown for ERA-Interim (top row) and the BOM, NCEP, and ECMWF hindcast simulations at target leads from 0 to 5 days (second, third, and fourth rows, respectively).

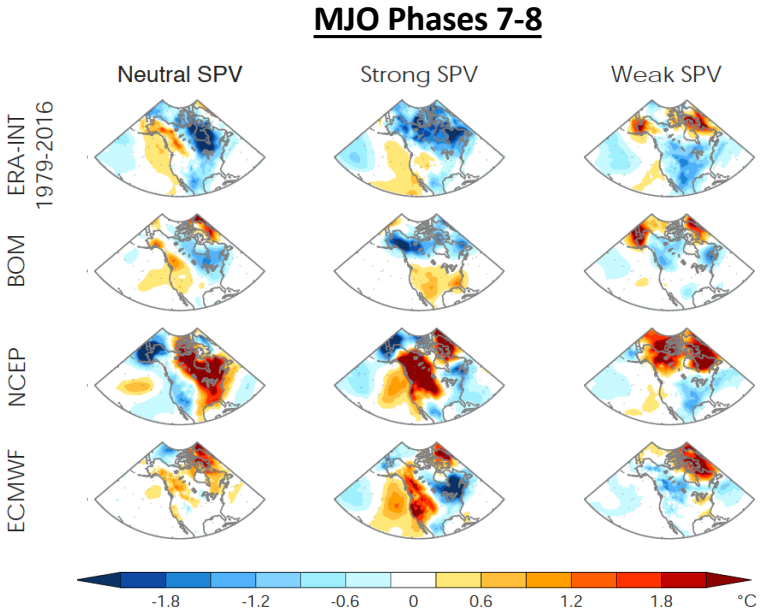

FIG. 15. As in **FIG. 14** but for times when the MJO is in Phases 7-8.

for MJO Phases 7-8, where convection is active in the Pacific and hence *closer* to North America, remains to be studied.

References

Cassou, C., 2008: Intraseasonal interaction between the Madden–Julian Oscillation and the North Atlantic Oscillation. *Nature*, **455**, 523–527. https://doi.org/10.1038/nature07286

Chu, T., and C. Glymour, 2009: Search for additive nonlinear time series causal models. *J. Mach. Learn. Res.*, **9**, 967–991.

Dee, D. P. et al., 2011: The ERA-Interim reanalysis: Configuration and performance of the data assimilation system, *Quart. J. Roy. Meteor. Soc.*, **137**, 553–597.

Ebert-Uphoff, I., and Y. Deng, 2012: Causal discovery for climate research using graphical models. *J. Climate*, **25**, 5648–5665.

Edmon, H. J., Hoskins, B. J., & McIntyre, M. E., 1980: Eliassen-Palm cross sections for the troposphere. *J. Atmos. Sci.*, **37**, 2600–2616.

Kiladis G. N., et al., 2014: A comparison of OLR and circulation based indices for tracking the MJO. *Mon. Wea. Rev.*, **142**, 1697-1715.

L'Heureux, M. L., and R. W. Higgins, 2008: Boreal winter links between the Madden–Julian Oscillation and the Arctic Oscillation. *J. Climate*, **21**, 3040–3050.

Runge, J., et al., 2015: Identifying causal gateways and mediators in complex spatio-temporal systems. *Nature Commun.*, **6**, 8502.

Thompson, D. W. J., and J. M. Wallace, 2000: Annular modes in the extratropical circulation. Part I: Month-to-month variability, *J. Climate*, **13**, 1000–1016.

Thompson, D. W. J., Furtado, J. C., & Shepherd, T. G., 2006: On the tropospheric response to anomalous stratospheric wave drag and radiative heating. *J. Atmos. Sci.*, **63**, 2616–2629.

Vitart, F., 2017: Madden–Julian oscillation prediction and teleconnections in the S2S database. *Quart. J. Roy. Meteor. Soc.*, **143**, 2210–2220.

Vitart, F., et al., 2017: The Subseasonal to Seasonal (S2S) Prediction project database. *Bull. Amer. Meteor. Soc.*, **98**, 163–173.

Wheeler, M.C. and H.H. Hendon, 2004: An all-season real-time multivariate MJO index: Development of an index for monitoring and prediction. *Mon. Wea. Rev.,* **132**, 1917–1932.

4. Highlights of Accomplishments

Task #1

- Composite results from ERA-Interim reanalysis support the proposal's central hypothesis – i.e., there are demonstrable spatial and amplitude differences in the NH teleconnected responses when considering MJO-SPV joint composites versus the composites of each mode separately.
- The state of the SPV exerts a more dominant control of the Atlantic / European sector longwave and sensible weather patterns irrespective of the phase of the MJO. By contrast, for the Pacific sector and western North America, the phase of the MJO dominates subseasonal weather influences more than the SPV. The rest of North America remains variable, and conditions depend more on both the MJO **and** the SPV. (**Figs. 2** and **4**).
- The impacts of the MJO on the tropospheric circulation (i.e., as characterized by the state of the tropospheric NAM / NAO) can occur either via a tropospheric-only pathway or a

stratospheric pathway, dependent on the phase of the MJO (**Figs. 5-7**). These pathways were reconfirmed using causal discovery theory (**Fig. 10**). As such, we have gained both a dynamical understanding of the connections associated with the MJO-stratosphere modulation hypothesis *and* an actual application of this hypothesis for winter weather regimes and S2S forecasting.

Task #2

- The S2S models investigated in this work perform well at recovering the observed MJO-tropospheric NAM connections, but struggle with MJO long-lead forecasts (**Fig. 11c**).
- Issues arise with the MJO-stratosphere linkages in the S2S models (**Fig. 12**), which may be the result of poor stratospheric resolution or missing stratosphere-troposphere dynamics. However, the models have better representation of teleconnections during MJO Phases 2-4 with any phase of the SPV (**Fig. 14**), possibly highlighting biases in the model with tropical convection.

5. Transitions to Applications

No formal transition to applications was performed with this work.

6. Publications from the Project

Barnes, E., I. Ebert-Uphoff, S. Samarasinghe and J. C. Furtado, 2019: Tropospheric and stratospheric causal pathways between the MJO and NAO. *J. Geophys. Res. Atmos.*, **124**, 9356-9371, doi:10.1029/2019JD0310254.

Green, M. R., and J. C. Furtado: Evaluating the joint influence of the Madden-Julian Oscillation and the stratospheric polar vortex on weather patterns in the Northern Hemisphere. *J. Geophys. Res. Atmos.*, **124**, 11693–11709, https://doi.org/10.1029/2019JD030771.

The following publication was submitted and returned with major revisions. However¸ the CPC authors have not re-submitted the manuscript.

Ciasto, L. M., M. L'Heureux, and K. Harnos, 2020: Relationships between the MJO and the extratropical stratospheric circulation in the International S2S Database models. *J. Climate*, conditionally accepted pending major revisions.

7. PI Contact Information

Jason C. Furtado
University of Oklahoma School of Meteorology
120 David L. Boren Blvd. Suite #5900
Norman, OK 73072

Phone: +1-405-325-1391
Email: jfurtado@ou.edu